Astron. Astrophys. 313, 657–663 (1996)

ASTRONOMY AND ASTROPHYSICS

The excitation and abundance of HDO toward W 3(OH)/(H_2O)

F.P. Helmich[1,2], **E.F. van Dishoeck**[1,3], **and D.J. Jansen**[1]

[1] Leiden Observatory, P.O.-Box 9513, 2300 RA Leiden, The Netherlands
[2] SRON Laboratory Groningen, P.O.-box 800, 9700 AV Groningen, The Netherlands
[3] Visiting Associate, Division of Physics, Mathematics and Astronomy, California Institute of Technology, Pasadena CA 91125, USA

Received 15 November 1995 / Accepted 27 January 1996

Abstract. The HDO $1_{01} - 0_{00}$ ground-state line at 464 GHz has been detected toward the high-mass star-forming clumps W 3(OH) and W 3(H_2O), together with the higher-lying $2_{11} - 2_{12}$ and $3_{12} - 2_{21}$ lines at 241 and 225 GHz, respectively. A detailed analysis of the HDO excitation shows that the higher levels are most likely populated by intense far-infrared radiation due to warm dust. The data allow constraints on the dust temperature ($T_{dust} > 100$ K), total column of dust ($E(B-V) > 500$ mag) and HDO column density. Combined with $H_2^{18}O$ data recently obtained by Gensheimer et al. (1996), the deuteration of water is found to be lower than that of other species, [HDO]/[H_2O]=(2–6) 10^{-4}, but comparable to that found for other "hot cores".

Key words: ISM: molecules – ISM: clouds – ISM: individual: W 3(OH); W 3(H_2O) – radio lines:ISM

1. Introduction

Unlike water itself, HDO possesses a number of low excitation lines which can be observed from Earth and are not masing. Although HDO was discovered already in 1975 through observations of the $1_{10} - 1_{11}$ transition at 80.6 GHz (E_u = 47 K) (Turner et al. 1975), most recent work has focussed on the higher-lying $2_{11} - 2_{12}$ (E_u = 95 K), $3_{12} - 2_{21}$ (E_u = 168 K) and $4_{22} - 4_{23}$ (E_u = 319 K) lines at 241, 225 and 143 GHz, respectively (Jacq et al. 1988, 1990; Gensheimer et al. 1996). However, observations of the latter lines are biased toward high-temperature, high-density regions. In order to better constrain the HDO excitation and its abundance in the bulk of the gas, information on lower-lying lines in small beams is needed. Recent improvements in submillimeter receivers have allowed the detection of the ground-state $1_{01} - 0_{00}$ HDO line at 464 GHz at high angular resolution in Orion-KL, but searches for this line in other sources have so far proved elusive (Schulz et al. 1991). We report here the second detection of the 464 GHz line in two other high-mass star-forming clumps: W 3(OH) and W 3(H_2O). Together with data on the 225 and 241 GHz lines in a similarly small beam, this allows a detailed determination of the HDO excitation and abundance.

Send offprint requests to: F.P. Helmich

The HDO analysis is not only important by itself, but also permits constraints on the amount of deuterium fractionation of water, especially when combined with recent observations of the $H_2^{18}O$ $3_{13} - 2_{20}$ line at 203 GHz (E_u=194 K; Gensheimer et al. 1996). It is well known that the deuterated forms of species such as HCN (Mangum, Plambeck & Wootten 1991; Schilke et al. 1992), NH_3 (Walmsley et al. 1987) and CH_3OH (Mauersberger et al. 1988a; Schulz et al. 1991; Jacq et al. 1993) have much higher abundances in "hot core" type regions than expected on the basis of the cosmic [D]/[H] ratio of $\sim 1.6 \cdot 10^{-5}$. This has been interpreted in terms of evaporation of icy grain mantles in massive star-forming regions, where the deuterium fractionation results from a previous colder phase and from grain surface reactions (Tielens 1989, Brown & Millar 1989). An analysis of the type presented here will allow a more accurate determination of the HDO/H_2O ratio. A particularly interesting question is whether this ratio depends on the evolutionary state of the object, since it is expected to decline as soon as high-temperature gas-phase reactions become effective. For this reason, we have selected the W 3 region for observations, since it contains several high-mass star-forming clumps at different evolutionary phases for which detailed complementary information is available (Helmich et al. 1994; Wilson et al. 1991, Helmich & van Dishoeck 1996). Also, accurate HDO/H_2O abundance ratios have recently been determined for a number of other high-mass star-forming clumps by Gensheimer et al. (1996) for comparison.

2. Observations and results

The observations were made with the 15 m James Clerk Maxwell Telescope[1] (JCMT) on Mauna Kea, Hawaii. The measurements of the HDO 225, 241 and 464 GHz lines were taken between August 1992 and October 1995 as part of the line survey project of three sources in W 3: W 3 IRS4, W 3 IRS5 and W 3(H_2O). Because of their special interest, these lines were

[1] The James Clerk Maxwell Telescope is operated by the Observatories on behalf of the Particle Physics and Astronomy Research Council of the United Kingdom, the Netherlands Organisation for Scientific Research, and the National Research Council of Canada.

also observed toward W 3(OH), located $\sim 7''$ E of W 3(H_2O). All data were taken with the facility receivers A2 and C2, respectively. See Matthews (1995) and references therein for technical details. Typical system temperatures were 500–700 K at 230 GHz and $\sim$ 3000 K (June 1994) to $\sim$ 1000 K (December 1994) at 460 GHz. The main beam-efficiency at 230 GHz as measured on planets was only 0.5 in August 1992, but increased to 0.63 in July 1993. At 460 GHz, it was 0.45 in June 1994 and 0.5 in December 1994. The 225 and 241 GHz lines toward W 3(H_2O) and W 3(OH) were re-observed in October 1995 under excellent weather conditions, resulting in system temperatures of about 400 K. The beam-efficiency was 0.68. The integrated intensities of these lines agree within 20% with those obtained in earlier runs.

All data were taken in double side-band mode; for receiver A2, the lines were placed in the lower side band with the upper side band 3 GHz apart. For receiver C2, the 464 GHz line was placed in the upper side band, with the lower side band shifted by 7.88 GHz. As the backend, the 2048 channel acousto-optical spectrometer (AOSC) was used in August 1992, and the digital autocorrelation spectrometer (DAS) with different frequency resolutions in later runs (Matthews 1995). Line identification was performed with help of the JPL and Lovas catalogues (see Groesbeck 1994 for references). The image side bands were checked for possible blends, but no obvious candidates were found. Especially at 464 GHz, several possible overlapping lines of CH_3OH and SO_2 occur; different local oscillator settings were performed to assure that the line is not blended with lines from the image side-band. The 225 GHz line is slightly blended with a line of CH_3OCHO in the signal side band, but the contribution of methylformate to the integrated line intensity is found to be less than 20% from other components of this line seen in the same setting.

All observations were done in beam-switch mode with a throw of $+180''$ in azimuth. The pointing was checked on W 3(OH) every half hour at 460 GHz and every hour at 230 GHz, and was well within $3''$. The beam of the JCMT is $10.5''$ at 460 GHz and $20.8''$ at 230 GHz. The calibration was done in the standard way using the chopper-wheel method (see Kutner & Ulich 1981). The absolute calibration is estimated to be accurate to $\sim$30%, consistent with the variations found for the 225 and 241 GHz data between different runs.

Fig. 1 shows the observed spectra at 464 GHz toward W 3(OH) and W 3(H_2O) with the $1_{01} - 0_{00}$ HDO line indicated; the continuum emission of $\sim$0.8 K has been removed. Fig. 2 illustrates the 225 and 241 GHz spectra for these two sources from the October 1995 run.

Table 1 lists the results of Gaussian fits to the observed HDO lines. No HDO lines were detected at a convincing level toward W 3 IRS4 and IRS5, but the observing conditions toward the latter source at 464 GHz were not as good as toward the other two sources, so that the 2σ limit of < 0.5 K is less meaningful. The JCMT intensities for the 225 GHz lines toward W 3(H_2O) and W 3(OH) are a factor of ~ 2 lower than those of Jacq et al. (1990) obtained in a $12''$ beam with the IRAM 30m telescope, suggesting that the emission originates from a small source.

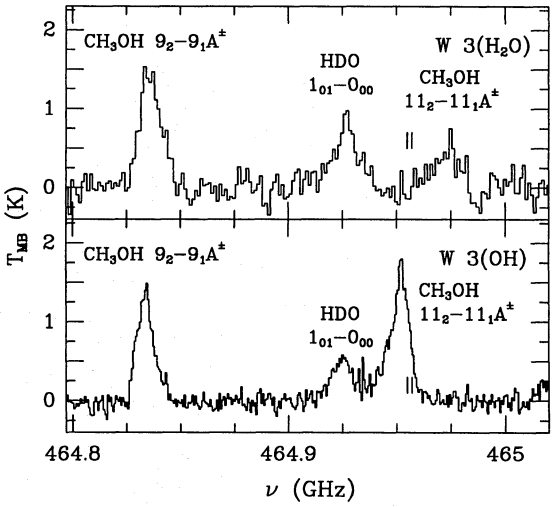

Fig. 1. Observed spectra toward W 3(H_2O) and W 3(OH), showing the detection of the HDO $1_{01} - 0_{00}$ 464 GHz line. The CH_3OH $11_2 - 11_1$ $A^{\pm}$ line originates in the upper (image) side band, whereas the other CH_3OH and the HDO lines are in the lower side band. The positions of two $^{34}SO_2$ lines ($29_{2,28} - 29_{1,29}$ and $10_{3,7} - 10_{0,10}$) are indicated by tick marks. Due to different atmospheric corrections, the intensity of the $11_2 - 11_1$ $A^{\pm}$ line toward W 3(H_2O) should be multiplied by 1.4. The two observations were done at slightly different LO settings, the lower side-band is centered at $V_{LSR} = -47$ km s^{-1}.

However, the 241 GHz line toward W 3(OH) is in good agreement with their measurements, although the data for this line are more noisy. Within the errors of both the IRAM and the JCMT calibration, the data could still be consistent with extended emission at this position. We will consider both options in the analysis. Jacq et al. (1990) also made a map of the 225 GHz line, which indicates that the emission peaks on W 3(H_2O); the contrast in the map is apparently small, however. Fits to lines of other species detected in the 225 and 241 GHz spectra are given in Helmich & van Dishoeck (1996).

The $1_{01} - 0_{00}$ line profile toward W 3(OH) is well fit by a single Gaussian, but that toward W 3(H_2O) shows evidence for two components: a broad component and a much weaker, narrower component. It is also interesting that both in our work and that of Jacq et al. the HDO lines toward W 3(OH) do not occur at the velocity $V_{LSR} = -44.5$ km s^{-1} characterizing the absorbing lines of NH_3, CH_3OH and OH toward this source, but at –47 to –49 km s^{-1}. This is the same velocity as that of most molecular lines found toward W 3(H_2O). Although the JCMT beam at 230 GHz is large enough to pick up some contaminating emission from this source, the 464 GHz beam and the IRAM 230 GHz beam of $\sim 12''$ should be able to largely separate the two sources.

3. Analysis

3.1. Rotation diagram

Fig. 3 presents the rotation diagrams for W 3(H_2O) and W 3(OH) respectively. Two cases are included for each source.

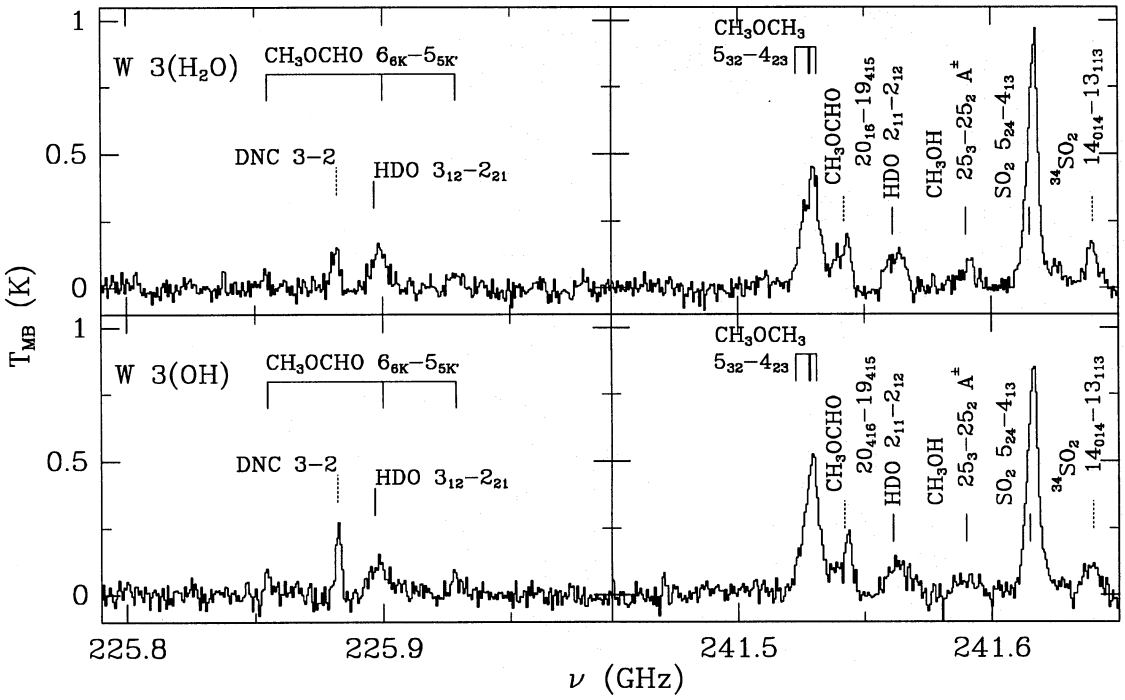

Fig. 2. Observed spectra toward W 3(H_2O) (upper panels) and W 3(OH) (lower panels), showing the HDO $3_{12}-2_{21}$ (left) and the $2_{11}-2_{12}$ line (right). The spectra are double side-band, centered on the HDO lines in the lower side band (at –47 km s^{-1}). Lines from the upper side-band are indicated by dotted tick marks.

The first result refers to the JCMT data only without correction for different beam sizes of the 460 and 230 GHz data, consistent with extended emission over ~20″ scales (solid line). The inferred T_{rot} is 93 ± 20 K for W 3 (H_2O) and 167 ± 50 K for W 3(OH), with HDO column densities of $\sim 210^{14}$ cm^{-2} in both sources. The second case is obtained by combining the 464 GHz JCMT line with the 225 GHz line measured by IRAM, and refers to a 12″ beam (dashed line). This plot also includes the upper limit at 143 GHz measured by Gensheimer et al. (1996). The resulting T_{rot} are increased to 160 ± 60 K for W 3(H_2O) and ~800 K for W 3(OH), with column densities of $\sim 510^{14}$ and $\sim 10^{15}$ cm^{-2}, respectively. Although the rotational temperatures are uncertain, especially for W 3(OH), it is clear that the HDO is highly excited in both sources.

3.2. *Excitation model*

In order to better determine the beam-averaged HDO column densities and the physical parameters of the gas in which it resides, statistical equilibrium calculations of the HDO excitation were performed. The calculations take the collisional and radiative (de-)excitation processes into account, and separate the level populations from the radiative transfer by means of an escape probability formulation. For a detailed description, see Jansen et al. (1994) and Jansen (1995). The HDO-He rate coefficients of Green (1989) were adopted.

In the case of W 3(H_2O), detailed knowledge about the physical and chemical conditions averaged over a 15″ beam is available from the analysis of the excitation of other molecules observed in the line survey (see Helmich et al. 1994; Helmich & van Dishoeck 1996). These data indicate T_{kin} = 220 K and $n(H_2)$ = 2 10^6 cm^{-3} on these scales. Interferometer observations of molecular and continuum emission by Turner & Welch (1984), Wink et al. (1994) and Wilner et al. (1995), however, indicate the presence of more compact clumps with sizes < 1″ to 5″ embedded in this core. The central unresolved clump seen in the continuum contains a young stellar object of spectral type B (Turner & Welch 1984; Wilner et al. 1995). Information on W 3(OH) can be found from data of Wilson et al. (1991) and Mauersberger et al. (1988b). This line of sight also samples the warm core with 100 K (Mauersberger et al. 1988b) and $n(H_2)$= 0.1 – 1 10^6 cm^{-3} (Wilson et al. 1991). Dense ($\sim 10^7$ cm^{-3}) embedded clumps of size 2-3″ are probably responsible for the OH maser emission at this position. The total beam-averaged (H_2) column densities are somewhat uncertain, but Helmich & van Dishoeck (1996) find $\sim 10^{23}$ cm^{-2} in a 15″ beam toward W 3(H_2O) from $C^{17}O$ 3–2 observations using $CO/H_2 = 3 \times 10^{-4}$ measured by Lacy et al. (1994) for dense, warm clouds. $C^{18}O$ 2–1 data by Wilson et al. (1991) suggest a value of $(1-3)10^{23}$ cm^{-2} in a 12″ beam toward W 3(OH), depending on the adopted CO/H_2 abundance. These values refer primarily to the core. The column densities for the compact clumps range from $\sim 10^{24}$ to 10^{25} cm^{-2}. Unfortunately, it is difficult to derive reliable column densities from (sub-)millimeter continuum data, because the dust emission is still overwhelmed by the free-free emission up to high frequencies, and most single dish data do not separate the two sources.

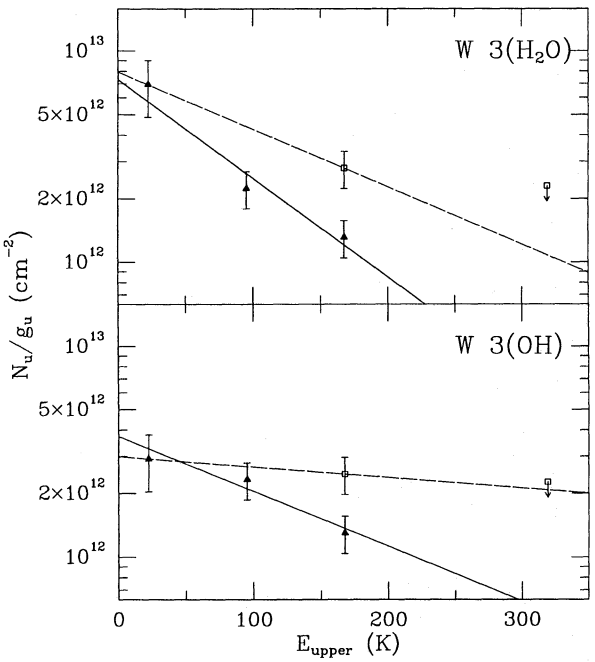

Fig. 3. Rotation diagrams for HDO toward W 3(H_2O) and W 3(OH). The open squares are the IRAM-data from Jacq et al. (1990) and Gensheimer et al. (1996). The solid triangles are the JCMT-data from this paper. The dashed line represents the fit of the JCMT 464 GHz line together with the IRAM data. The solid line represents the fit to the JCMT data only.

Table 1. HDO Line fitting parameters

Line	ν (GHz)	T_{MB} (K)	V_{LSR} (km/s)	ΔV (km/s)	$\int T_{MB} dV$ (K km/s)
		W 3(H_2O)			
$3_{12} - 2_{21}$	225.8967	0.14	–49.8	8.2	1.2
$2_{11} - 2_{12}$	241.5616	0.13	–48.4	8.8	1.2
$1_{01} - 0_{00}$	464.9245	0.97[1]	–48.6	8.1	8.4
		W 3(OH)			
$3_{12} - 2_{21}$	225.8967	0.10	–49.2	11.0	1.2
$2_{11} - 2_{12}$	241.5616	0.10	–49.1	11.3	1.2
$1_{01} - 0_{00}$	464.9245	0.48	–47.2	7.0	3.5
		W 3 IRS5			
$3_{12} - 2_{21}$	225.8967	<0.12[2,3]	–	–	–
$2_{11} - 2_{12}$	241.5616	<0.080[3]	–	–	–
$1_{01} - 0_{00}$	464.9245	0.46[4]	–39.3	4.1	2.0
		W 3 IRS4			
$3_{12} - 2_{21}$	225.8967	<0.060[3]	–	–	–
$2_{11} - 2_{12}$	241.5616	<0.074[3]	–	–	–

Coordinates (B1950.0): W 3(H_2O) $02^h\ 23^m\ 17\overset{s}{.}3$ $+61°38'58''$; W 3(OH) $02^h\ 23^m\ 16\overset{s}{.}45$ $+61°38'57\overset{''}{.}2$; IRS5 $02^h\ 21^m\ 53\overset{s}{.}1$ $+61°52'20''$; IRS4 $02^h\ 21^m\ 43\overset{s}{.}5$ $+61°52'49''$.

[1] If two components are fitted separately: T_{MB} = 0.55 K and ΔV = 10 km s^{-1}; and T_{MB} = 0.46 K and ΔV = 2.0 km s^{-1}.

[2] Unidentified line 2 MHz away.

[3] Upper limits are the rms noise in a 0.5 MHz channel.

[4] 2σ detection.

The excitation calculations have been performed for a range of densities and temperatures using initially only the cosmic background radiation field with T_{CBR} = 2.73 K. The resulting $1_{01} - 0_{00}/2_{11} - 2_{12}$ and $1_{01} - 0_{00}/3_{12} - 2_{21}$ line ratios are illustrated in Fig. 4a,c for the optically thin case. It is clear none of these calculations can reproduce the observed line ratios of < 10 for both sources: the differences are 2–3 orders of magnitude for $n(H_2) < 10^8$ cm^{-3}. Only for very high densities of $n(H_2) \approx 10^9$ cm^{-3} can the observed values be reproduced. It is, however, well known that light hydrides such as HDO are easily pumped by far-infrared radiation through their rotational lines (e.g., Churchwell et al. 1986; Moore et al. 1986, Jacq et al. 1990, Schulz et al. 1991). Since the W 3(OH)/(H_2O) region contains large amounts of warm dust and thus emits copious photons in the far-infrared (see e.g. Keto et al. 1992), this process is likely to be significant.

The far-infrared radiation field seen by the molecules is represented in our model by $I_\nu^b = B_\nu(T_{CBR}) + \eta_d B_\nu(T_{dust})(1 - \exp(-\tau_d))$, where $B_\nu(T_{dust})$ is the Planck function at the dust temperature T_{dust}, τ_d is the dust optical depth and η_d a geometrical dilution factor, which is taken to be 1. The dust opacity τ_d is computed by specifying a total column of dust in terms of $E(B-V)$ and using an opacity law of the form $\tau_\nu \propto \nu^\beta$ at $\lambda > 40$ μm which joins smoothly with the average interstellar extinction curve of Becklin et al. (1978) at shorter wavelengths. Theoretical models suggest β to be between 1 and 2. Measurements by Chini et al. (1986) indicate β to be 2.0 ± 0.4 for this region, a value which is consistent with the (uncertain) determination by Wilner et al. (1995) for W 3(H_2O). Because lower values of β cannot be excluded a priori, β = 1.5 is used in this work unless stated otherwise. The total beam-averaged column-density $N(H_2)$ is related to the extinction $E(B-V)$ through $N(H_2) = 2.4 \cdot 10^{21} E(B-V)$ cm^{-2}, assuming the amount of atomic hydrogen is negligible (Bohlin et al. 1983).

Toward W 3(OH), the free-free radiation from the H II region can also affect the excitation. This contribution was taken into account using T_{el} = 8400 K and an emission measure of 6.75 10^8 cm^{-6}pc (Baudry et al. 1993). Its influence turns out to be negligible for small (< 200) line ratios, however.

The resulting line ratios for a range of T_{dust} and $E(B-V)$ with β = 1.5 are presented in Fig. 4b,d, using T_{kin} = 220 K and $n(H_2) = 2\ 10^6$ cm^{-3}. Note that the results are not sensitive to the adopted kinetic temperature and density but differ by factors of a few if β = 2 or β = 1 is taken, the shape of the contours remaining the same. It is clear that both line ratios are smaller by 2-3 orders of magnitude if the far-infrared radiation is included and are within the range of observed values. Thus, these calculations can in principle be used to constrain both T_{dust} and $E(B-V)$. However, several other factors affect the interpretation, the most important of which are the adopted source size and source structure.

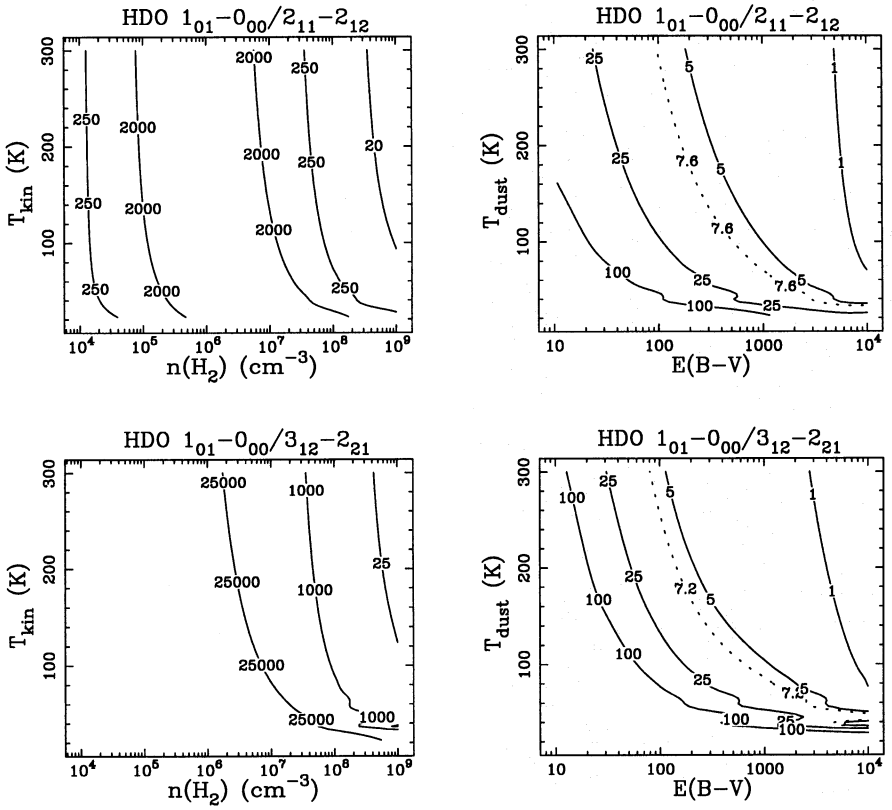

Fig. 4. HDO line ratios as functions of total number density and kinetic temperature (**a,c**) left panels, no dust, or as functions of reddening and dust temperature (**b,d**) right panels, $n(H_2) = 2\,10^6$ cm^{-3},T_{kin} = 220 K. The calculations refer to optically thin lines. The dotted line represents the observed ratio for W 3(H_2O) uncorrected for possible beam dilution.

3.3. Results

Consider first the case that the emission from W 3(OH) fills both the 230 and 460 GHz JCMT beam. Then the $1_{01}-0_{00}/2_{11}-2_{12}$ and $1_{01}-0_{00}/3_{12}-2_{21}$ line ratios are $\sim$ 3. This implies $T_{dust} > 100$ K and $E(B-V) > 1000$. The line ratio excludes $T_{dust} < 50$ K, but an upper limit on the dust temperature cannot be derived from these data. Because the inferred gas temperatures are 100-250 K, a dust temperature in this range is reasonable at these high densities. For T_{dust} = 150 K, $E(B-V) \approx 1000-2000$ magnitudes is found, or equivalently $N(H_2) = (2-5)10^{24}$ cm^{-2}, assuming diffuse cloud values for the relation between extinction and total column density. The beam-averaged column density N(HDO)$\approx 4.3\,10^{14}$ cm^{-2}, and the corresponding HDO/H_2 abundance $8\,10^{-11}$. This value must be regarded as a lower limit, however, since the total column density of the extended core is more likely that derived from $C^{18}O$ of $\sim 2\,10^{23}$ cm^{-2} giving a HDO abundance of $2\,10^{-9}$ (see Sect. 4). Using $\beta = 2$ results in $E(B-V) = 3000$, $T_{dust} = 200$ K and N(HDO) = $3.2\,10^{14}$ cm^{-2}. The excitation temperatures of the observed HDO lines range from 70 to 190 K in the model, indicating that the assumption of LTE used in the rotation diagram method is not quite valid.

For W 3(H_2O), the observed $1_{01}-0_{00}/2_{11}-2_{12}$ and $1_{01}-0_{00}/3_{12}-2_{21}$ ratios are $\sim$ 8, which indicates $T_{dust} \approx 100$ K and $E(B-V) \approx 500$ magnitudes. This would imply a total H_2 column density of $\sim 10^{24}$ cm^{-2}. From the absolute strengths of the lines a beam-averaged HDO column density of $2\,10^{14}$ cm^{-2} is obtained. For β = 1 or 2, the HDO column density is not changed, but the dust parameters vary by a factor of three.

As mentioned in Sect. 2, comparison of the JCMT and IRAM 225 GHz data suggests that for both sources, but in particular W 3(H_2O), the source size is small, only a few arcseconds. This would be consistent with interferometer observations of other "hot core" molecular species like HCN and CH_3CN toward W 3(H_2O), which show a typical source size of $< 1.2''$ (Wink et al. 1994; Turner & Welch 1984). If we take the 225 GHz values for W 3(H_2O) from both telescopes at face value, the difference implies a source size of 3.5″, comparable to the 5″ clump found from HCO^+ and $C^{18}O$ by Wink et al. (1994). The single-dish measurements are not sensitive to emission coming from the smallest scales ($\sim 1''$), but can easily pick up emission from the intermediate (5″) scales. Moreover, the dust continuum from the compact ($<1''$) source is optically thick at wavelengths shorter than 1 mm, so that the 464 GHz line must originate from a larger region. Therefore 5″ was adopted as the source size for the HDO emission. This implies that the line ratios decrease from $\sim$8 to $\sim$2, so that the inferred $E(B-V)$ and T_{dust} for W 3(H_2O) increase, and become similar to those found for W 3(OH). The absolute strengths of the lines corrected for beam-dilution give N(HDO) = $5\,10^{15}$ cm^{-2}. The optical depth in the ground state line is $\sim$0.1, and the 230 GHz lines are optically thin. The optical depth for the 464 GHz line is much lower than that found for Orion by Schulz et al. (1991), but it depends strongly on the source size. If the source of HDO emission is less than $\sim 5''$, the ground state 464 GHz line will rapidly get optically thick. This has the effect of shifting the curves in Fig. 4 to lower $E(B-V)$.

If β = 1 or 2 is used, the same HDO column density is obtained, but the dust parameters vary a factor three at most. Thus, in spite of the uncertainties in the data and models, the column density of HDO can be determined fairly well, the major uncertainty being the source size. The inferred dust column density and its associated temperature are more uncertain, since only the total radiative excitation rates (i.e., the number of pumping photons) in the 0.8–3 THz range are constrained by the observed line ratios. Different choices of β therefore necessitate different values of $T_{\rm dust}$ and $E(B-V)$ within the adopted model.

The above analysis assumes that all of the HDO emission arises from a single component. As discussed in Sect. 2, the $1_{01} - 0_{00}$ line profile toward W 3(H_2O) shows some evidence for two components. The narrower component probably arises in the core surrounding also W 3(OH), which fills a significant part of the beam. The broader, dominating, component would then originate in the 5″ clump seen in the interferometer in other species. Higher spatial resolution and higher signal-to-noise data are needed to do a proper decomposition, and to determine the relative amount of HDO in these components.

Some high-mass star-forming cores such as SgrB2 are known to have cold, low density envelopes surrounding them. In these cases, the ground state lines of hydrides such as NH_2 (van Dishoeck et al. 1993), HCl and $H_2{}^{18}O$ (Zmuidzinas et al. 1995, 1996) are readily seen in absorption rather than emission. Could the strength of the 464 GHz emission be affected by such absorption? In the case of the W 3(OH)/W 3(H_2O) region, there is no evidence for a massive cold envelope from observations of other lines. Absorption lines of NH_3, CH_3OH and other species are seen at longer wavelengths against the free-free continuum of W 3(OH), but this gas is warm. Also, the absorption velocity of –44.5 km s^{-1} is well separated from the –49 km s^{-1} emission observed in this work. Moreover, the presence of a lower density envelope containing HDO should not affect the 464 GHz emission if the density is below the critical density in the envelope. In this case the envelope acts as a "diffuse scatterer" rather than a true absorber, so that the total number of photons is conserved (Zmuidzinas et al. 1996).

For W 3 IRS5, $n(H_2)$ = 1 10^6 cm^{-3} and $T_{\rm kin}$ = 100 K (Helmich et al. 1994) has been found. Because the 225 and 241 GHz lines are not detected, no useful constraints on the dust parameters can be obtained from the HDO line ratios. The upper limits imply $E(B-V)$ <1000 mag. For $T_{\rm dust}$ = 65 K (Gordon 1987), $E(B-V)$ = 300 mag, the 2σ detection of the 464 GHz ground state line then implies N(HDO) = 2 10^{13} cm^{-2}, which is uncertain by a factor of a few. Combined with an estimated H_2 column density from $C^{17}O$ 3–2 of 10^{23} cm^{-2}, this implies an HDO abundance of 210^{-10}. No useful HDO limits can be obtained toward W 3 IRS4.

4. Discussion

The HDO molecule is not only of chemical interest, but it also offers a fascinating excitation puzzle. From Sect. 3, it is clear that if the excitation is caused by far-infrared radiation, the HDO molecules are exposed to radiation from a very large column ($E(B-V) \approx$ 1000 mag) of warm dust ($T_{\rm dust}$ > 100 K). This calculation assumes, however, that the HDO molecules and the dust are well mixed. The large inferred (beam-averaged) column densities of > 10^{24} cm^{-2} are consistent with the high values found for the more compact clumps toward W 3(H_2O) (Wink et al. 1994; Wilner et al. 1995), but are an order of magnitude larger than those derived for the core on 12″ scales. Since the data indicate that at least some HDO is present in the core, it is likely that these molecules are excited primarily by the continuum radiation from the compact clumps, albeit with some geometrical dilution. More detailed modeling requires information on the HDO and dust distribution at arcsec resolution.

The detection of vibrationally excited CS and HCN toward W 3(H_2O) (Helmich & van Dishoeck 1996) strengthens the argument for a large column of warm dust at high temperature, emitting enough photons to pump even the vibrational lines of these species at 8 and 13 μm, respectively. Approximately 10% of the dust column necessary for the HDO excitation must be at a temperature of more than 500 K to explain the vibrationally excited CS emission. Thus, this emission must originate very close to the young stellar object.

Toward W 3(OH), the very low $1_{01} - 0_{00}/2_{11} - 2_{12}$ and $1_{01} - 0_{00}/3_{12} - 2_{21}$ line ratios and the large inferred $E(B-V)$ remain puzzling. The corresponding high excitation temperatures of ~800 K may indicate that some shock excitation, for example in the dense clumps also responsible for the OH masers, plays a role as well. The broader line profiles of ~11 km s^{-1} would be consistent with this interpretation. Deeper searches for even higher excitation HDO lines at this position will be valuable, but difficult with current instrumentation.

The recent $H_2^{18}O$ measurements toward W3 made by Gensheimer et al. (1996) allow the deuteration of water to be determined. If we assume that the HDO is well mixed with the H_2O, we can apply the same physical conditions (with β = 1.5) as found for HDO to determine the column densities of $H_2^{18}O$. The H_2O column densities are then calculated using an ortho/para ratio of 3:1 and an [H_2O]/[$H_2^{18}O$] ratio of 500. Due to the different assumptions, our H_2O column densities differ by ~20% from those of Gensheimer et al. (1996). For W 3(OH) 2.2 10^{18} cm^{-2} is found and for W 3(H_2O) 1.4 10^{18} cm^{-2} in the beam-filling case, or 8.6 10^{18} cm^{-2} if the emission comes from a 5″ region. The [HDO]/[H_2O] ratio is then 2 10^{-4} for W 3(OH) and (2 – 6) 10^{-4} for W 3(H_2O). Unfortunately, no similar data are available for W 3 IRS5 to determine its [HDO]/[H_2O] ratio, even though H_2O is definitely present in that source as well (Cernicharo et al. 1990; Phillips et al. 1992).

Despite the uncertainties in observations, assumptions and models, the derived [HDO]/[H_2O] ratios are a robust and striking result. The values are very similar to the [HDO]/[H_2O] ratios found for other "hot cores" by Gensheimer et al. (1996), but are lower than the deuteration ratios of other species. For example, for W 3(H_2O) Helmich & van Dishoeck (1996) find the deuteration for HCO^+, HCN and HNC to be 4 10^{-3}, 8 10^{-3} and 4 10^{-3} respectively. Compared with these values, H_2O is only moderately deuterated, even if the emission stems from the 5″ region.

Current scenarios (see e.g. Tielens 1989; Millar et al. 1989; Brown & Millar 1989) suggest that the high deuteration originates in the chemistry at very low temperatures earlier in the history of the cloud. The molecules will subsequently stick on the dust grains, forming icy dust-mantles, in which the high deuteration is preserved and enhanced through grain surface reactions with atomic deuterium. After evaporation of these ice-mantles in a warmer phase, the gas-phase is enriched with high abundances of deuterated species. In the subsequent (high-temperature) chemistry the deuteration is gradually removed. One might thus have expected to see a difference in the amount of deuteration for the two sources studied here: the deuteration should have been higher toward the young source W 3(H_2O) than toward the older W 3(OH), whereas the W 3 IRS5 ratio should have been even higher. The lack of evidence, and the remarkably narrow range of observed [HDO]/[H_2O] in other regions, suggest that other factors play a role as well. If gas-phase processes are dominant, the deuterium fractionation of H_2O results mostly from reactions with H_2D^+, whereas that of HCN and HNC stems from the CH_2D^+ route (Millar et al. 1989). The former route is particularly enhanced at low temperatures, <30 K, whereas the second route is still effective up to ~70 K. Thus, one possible explanation for the observed difference in fractionation between H_2O and HCN is that the cloud stayed warm (>50 K) during its entire evolution and never went through a very cold phase. Other explanations include the possibility that HDO and H_2O are currently located in a different, warmer region from other deuterated species such as DCN and CH_3OD, and/or that the HDO/H_2O ratio is returned faster to a steady-state situation than the other deuteration ratios due to some as yet unidentified reaction.

5. Conclusions

Observations of the HDO 464 GHz ground state line have been made toward the W 3(OH)/(H_2O) region. Together with complimentary information from higher energy lines, the total column of dust, the dust temperature and the beam-averaged HDO column density can be constrained. The HDO is likely present in both the extended core surrounding the W 3(OH)/H_2O region, and in the dense, compact clumps. The intense far-infrared radiation field from the clumps can excite the HDO, also in the core. The inferred HDO column densities are well determined, but the abundances are more uncertain. Together with the data of Gensheimer et al. 1996 on $H_2^{18}O$, the [HDO]/[H_2O] ratio is determined to be $(2-6)10^{-4}$, similar to that found in other "hot cores". This suggests that the [HDO]/[H_2O] ratio is not a sensitive indicator of evolutionary stage of the object.

Acknowledgements. The authors thank Michiel Hogerheijde and Remo Tilanus for performing part of the observations. The JCMT staff is acknowledged for their fine support. Paul Gensheimer provided his results prior to publication. This work benefitted from discussions with John Black and Jonas Zmuidzinas. EvD and FPH are grateful to the Netherlands Organization for Pure Research (NWO) for support through a PIONIER grant. EvD also acknowledges the hospitality of the California Institute of Technology, where part of this work was performed.

References

Baudry, A., Menten, K.M., Walmsley, C.M., Wilson, T.L., 1993, A&A 271, 552
Becklin, E.E., Matthews, K., Neugebauer, G., Willner, S.P., 1978, ApJ 220, 831
Bohlin, R.C., Hill, J.K., Jenkins, E.B. et al., 1983, ApJS 51, 277
Brown, P.D., Millar, T.J., 1989, MNRAS 237, 661
Cernicharo, J., Thum, C., Hein, H. et al., 1990, A&A 231, L15
Chini, R., Krügel, E., Kreysa, E., 1986, A&A 167, 315
Churchwell, E., Wood, D., Myers, P.C., Myers, R.V., 1986, ApJ 305, 405
Gensheimer, P.D., Mauersberger, R., Wilson, T.L., 1996, A&A in press
Gordon, M.A., 1987, ApJ 316, 258
Green, S. 1989, ApJS 70, 813
Helmich, F.P., Jansen, D.J., de Graauw, Th. et al., 1994, A&A 283, 626
Groesbeck, T.D., 1994, PhD thesis California Institute of Technology
Helmich, F.P., van Dishoeck, E.F., 1996, A&AS (in preparation)
Jacq, T., Jewell, P.R., Henkel, C., Walmsley, C.M., Baudry, A., 1988, A&A 199, L5
Jacq, T., Walmsley, C.M., Henkel, C. et al., 1990, A&A 228, 447
Jacq, T., Walmsley, C.M., Mauersberger, R. et al., 1993, A&A 271, 276
Jansen, D.J., van Dishoeck, E.F., Black, J.H., 1994, A&A 282, 605.
Jansen, D.J., 1995, Thesis University of Leiden
Keto, E., Proctor, D., Ball, R., Arens, J., Jernigan, G., 1992, ApJ 401, L113
Kutner, M.L., Ulich, B.L. 1981, ApJ 250, 341
Lacy, J.H., Knacke, R., Geballe, T.R., Tokunaga, A.T. 1994, ApJ 428, L69
Mangum, J.G., Plambeck, R.L., Wootten, A., 1991, ApJ 369, 169
Matthews, H.E., 1995, in: The James Clerk Maxwell Telescope: a Guide for the Prospective User
Mauersberger, R., Henkel, C., Jacq, C., Walmsley, C.M., 1988a, A&A 194, L1
Mauersberger, R., Wilson, T.L., Henkel, C., 1988b, A&A 201, 123
Millar, T.J., Bennett, A., Herbst, E., 1989, ApJ 340, 906
Moore, E.L., Langer, W.D., Huguenin, G.R., 1986, ApJ 306, 682
Phillips, T.G., van Dishoeck, E.F., Keene, J., 1992, ApJ 399, 533
Schilke, P., Walsmley, C.M., Pineau des Forêts, G. et al., 1992, A&A 256, 595
Schulz, A., Güsten, R., Serabyn, E., Walmsley, C.M., 1991, A&A 246, L55
Tielens, A.G.G.M., 1989, in Interstellar Dust, IAU Symposium 135, ed. L.J. Allamandola & A.G.G.M. Tielens (Dordrecht: Kluwer), p. 239
Turner, B.E., Zuckerman, B., Fourikis, N., Morris, M., Palmer, P., 1975, ApJ 198, L125
Turner, J.L., Welch, W.J., 1984, ApJ 287, L81
van Dishoeck, E.F., Jansen, D.J., Schilke, P., Phillips, T.G., 1993, ApJ 416, L83
Walmsley, C.M., Hermsen, W., Henkel, C., Mauersberger, R., Wilson, T.L., 1987, A&A 172, 311
Wilner, D.J., Welch, W.J., Forster, J.R., 1995, ApJ 449, L73
Wilson, T.L., Johnston, K.J., Mauersberger, R., 1991, A&A 251, 220
Wink, J.E., Duvert, G., Guilloteau, S. et al., 1994, A&A 281, 505
Zmuidzinas, J., Blake, G.A., Carlstrom, J., Keene, J., Miller, D., 1995, ApJ 447, L125
Zmuidzinas, J., Blake, G.A., Carlstrom, J. et al., 1996, ApJ in press

This article was processed by the author using Springer-Verlag LaTeX A&A style file version 3.